# Comprehensive ESR study of the antiferromagnetic ground states in the one-dimensional spin systems (TMTSF)2PF6, (TMTSF)2AsF6, and (TMTTF)2Br

**Michael Dumm, Alois Loidl, B. Alavi, K. P. Starkey, L. K. Montgomery, Martin Dressel**

**Angaben zur Veröffentlichung / Publication details:**

Dumm, Michael, Alois Loidl, B. Alavi, K. P. Starkey, L. K. Montgomery, and Martin Dressel. 2000. "Comprehensive ESR study of the antiferromagnetic ground states in the one-dimensional spin systems (TMTSF)2PF6, (TMTSF)2AsF6, and (TMTTF)2Br." *Physical Review B* 62 (10): 6512–20. https://doi.org/10.1103/PhysRevB.62.6512.



# Comprehensive ESR study of the antiferromagnetic ground states in the one-dimensional spin systems $(TMTSF)_2PF_6$, $(TMTSF)_2AsF_6$, and $(TMTTF)_2Br$

M. Dumm* and A. Loidl
*Experimentalphysik V, Universität Augsburg, Universitätsstrasse 2, D-86135 Augsburg, Germany*

B. Alavi
*Department of Physics, University of California, Los Angeles, California 90095-1547*

K. P. Starkey and L. K. Montgomery
*Department of Chemistry, Indiana University, Bloomington, Indiana 47405*

M. Dressel
*1. Physikalisches Institut, Universität Stuttgart, Pfaffenwaldring 57, D-70550 Stuttgart, Germany*
(Received 19 January 2000; revised manuscript received 14 April 2000)

Detailed electron spin resonance experiments have been performed on single crystals of $(TMTSF)_2PF_6$, $(TMTSF)_2AsF_6$, and $(TMTTF)_2Br$. These low-dimensional organic compounds undergo transitions to incommensurate and commensurate antiferromagnetic ground states, respectively. From the antiferromagnetic resonances observed at low temperatures we obtain information on the anisotropy energies, the zero-field spin-wave frequency, and the spin-flop field. The anisotropy energies of the different AFM ground states depend strongly on the spin-orbit coupling constant of selenium or sulfur. Well below the phase transition, the order parameter of $(TMTSF)_2PF_6$ and $(TMTSF)_2AsF_6$ is only weakly temperature dependent indicating visible deviations from the behavior expected in mean-field theory. In contrast, the sublattice magnetization of $(TMTTF)_2Br$ is a function of temperature down to 4.2 K suggesting the excitation of thermal magnons. The temperature dependence of the spin susceptibility in the paramagnetic state can be described by the Hubbard model in the limit of strong Coulomb repulsion. Near the phase transitions the spin dynamics are characterized by antiferromagnetic fluctuations.

## I. INTRODUCTION

The linear-chain compounds $(TMTSF)_2X$ and $(TMTTF)_2X$, where TMTSF is tetramethyltetraselenafulvalene, TMTTF is tetramethyltetrathiafulvalene, and $X$ stands for a monovalent anion such as $AsF_6$, $PF_6$, $ClO_4$, and Br, are considered as an ideal class of low-dimensional systems to study the crossover from localized to itinerant spins and charges.[1–3] The sulfur salts are Mott insulators with localized spins while the Bechgaard salts $(TMTSF)_2X$ are quasi one-dimensional metals. Depending on the organic molecule TMTSF or TMTTF and/or the anion $X$, phase transitions in different ground states are observed at low temperatures $T \leqslant 20$ K.

$(TMTSF)_2PF_6$ and $(TMTSF)_2AsF_6$ are still regarded as the prime examples of one-dimensional spin-density-wave (SDW) systems.[1,4] This insulating state is a consequence of the instability of the quasi one-dimensional Fermi surface and can be considered as an itinerant antiferromagnet.[4] A large number of experimental investigations have been dedicated to the nonlinear transport and optical properties of the SDW ground state.[5,6] The magnetic properties have been subject to investigations by nuclear magnetic resonance (NMR) (Refs. 7,8) and muon spin relaxation ($\mu$SR).[9] In these experiments, distinct deviations from the behavior predicted by the mean-field theory were found in the temperature dependence of the order parameter of $(TMTSF)_2PF_6$. Since early experiments,[10–15] susceptibility and electron spin resonance (ESR) methods have only rarely been used to systematically explore the nature of this broken symmetry ground state although the appearance of antiferromagnetic resonances (AFMR) is one of the clearest signatures of the antiferromagnetic ordering.[16,17] For example, no work on AFMR of $(TMTSF)_2PF_6$ has been published up to now. It is known from NMR that the SDW ground state in $(TMTSF)_2PF_6$ has an incommensurate wave vector $\vec{Q} = (0.5,0.24,0.06)$ and an amplitude of $\mu = 0.08\mu_B$.[18] In a number of recent experimental works the coupling of the SDW to the lattice is subject to discussion.[6,19] X-ray diffuse scattering experiments gave indications of a mixture between a spin-density and a charge-density wave (CDW) in the ground state of $(TMTSF)_2PF_6$.[20] Above the transition in the SDW ground state, the Bechgaard salts are highly anisotropic conductors. The electrodynamics of the metallic state are still of highest interest since the reduced dimensionality implies deviation from the Fermi-liquid picture.[21,22]

The charge carriers of the sulfur salts $(TMTTF)_2X$ on the other side, are stronger localized. The spin dynamics of these systems can be described by a $S = 1/2$ antiferromagnetic (AFM) Heisenberg chain in the high-temperature range.[3] While most (TMTTF) salts such as $(TMTTF)_2PF_6$ undergo a spin-Peierls transition at low temperatures, $(TMTTF)_2Br$ orders antiferromagnetically with a commensurate wave vector $\vec{Q} = (0.5,0.25,0)$ and a magnetic moment $\mu = 0.14\mu_B$ as determined by $^1$H-NMR investigations.[23] The commensurability of the wave vector is due to the fact that the antiferromagnetic order is induced by exchange interaction between

 

TABLE I. List of the characteristic parameters measured in different organic linear-chain compounds of TMTTF and TMTSF which exhibit an antiferromagnetic phase transition. $T_{SDW}$ and $T_N$ denote the transition temperatures to the spin-density-wave and antiferromagnetic ground state, $\nu$ is the microwave frequency, $\Omega_{\pm}$ are the frequencies of the zero-field modes, $H_{sf}$ indicates the spin-flop field, $J$ the exchange constant, and $D$ and $E$ the anisotropy energies.

| | $(TMTSF)_2X$ | | | | $(TMTTF)_2X$ | | | |
|---|---|---|---|---|---|---|---|---|
| $X$ | $PF_6$ | $AsF_6$ | | $ClO_4$ | Br | | SCN | $SbF_6$ |
| $T_{SDW}$ (K) | 12.2 | 12.2 | 12.5 | 6.0 | | | | |
| $T_N$ (K) | | | | | 13.8 | 13.0 | 8.8 | 6.0 |
| $\nu$ (GHz) | 9.1 | 9.1 | 35.3 | 11.4,17 | 9.5 | 9.3 | 9.3 | 9.3 |
| $\Omega_-$ (GHz) | 12.5 | 11.7 | 12.3 | 8.7 | 12.0 | 11.9 | 12.3 | 8.1 |
| $\Omega_+$ (GHz) | 36.9 | 34.6 | 35.3 | | 20.1 | 18.5 | 20.5 | 13.9 |
| $H_{sf}$ (kOe) | 4.5 | 4.2 | 4.4 | 3.1 | 4.3 | 4.3 | 4.6 | 3.3 |
| $J$ (K) | 1400 | 1400 | | | 500 | | | |
| $D$ (K) | 0.33 | 0.29 | | | 0.078 | | | |
| $E$ (K) | 0.02 | 0.018 | | | 0.017 | | | |
| Ref. | this work | | 16 | 17 | this work | 26 | 27 | 27 |

the spin chains with Mott-Hubbard localized charge carriers rather than by an instability of the quasi one-dimensional Fermi surface.[24] Additionally, the ground-state properties of $(TMTTF)_2Br$ were investigated by susceptibility[25] and AFMR (Ref. 26) measurements. A summary of the most relevant results of the previous AFMR measurements on $(TMTSF)_2AsF_6$ and $(TMTTF)_2Br$ as well as related compounds is given in Table I.

In this paper we present a detailed analysis of our new ESR measurements on $(TMTSF)_2PF_6$, $(TMTSF)_2AsF_6$, and $(TMTTF)_2Br$ in the temperature range 1.5 K$\leqslant T\leqslant$300 K. The purpose of our study is to investigate the magnetic properties of the different antiferromagnetically ordered states. Particularly, we will discuss the temperature dependences of the order parameter in $(TMTSF)_2X$ and $(TMTTF)_2Br$ and describe the influence of the relaxation processes on the anisotropy of the AFM states. To give a profound basis for the understanding of the influences of the spin-phonon and dipole-dipole coupling on the ground-state properties, we first discuss the regime of AFM fluctuations and present results on the high-temperature properties of $(TMTSF)_2AsF_6$.

## II. EXPERIMENTAL

Single crystals of $(TMTSF)_2PF_6$ and $(TMTSF)_2AsF_6$ were grown by using the standard electrochemical method.[10] The compounds are well characterized by transport measurements and show a metal-to-insulator transition at $T_{SDW}=12$ K. $(TMTTF)_2Br$ was synthesized electrochemically following a detailed procedure outlined previously.[28] The sizes of the single crystals were up to $4\times0.8\times0.7$ mm$^3$ for the $a$, $b$, and $c$ directions. The electron spin resonance experiments were performed in two conventional ESR spectrometers (Varian E-101 and Bruker Elexsys 500 CW) at 9.1 and 9.5 GHz for temperatures 1.5 K$\leqslant T\leqslant$300 K and magnetic field sweeps from $0\leqslant H\leqslant$19 kOe. The modulation frequency was 100 kHz. For cooling the sample down to 4.2 K, we used an Oxford He-flow cryostat; lower temperatures were achieved by utilizing a He bath cryostat. The single crystals were glued to a quartz rod by paraffin in order to ensure good thermal contact.They were oriented along their $a$, $b'$, or $c^*$ axes with an accuracy of $\pm5°$ by using a microscope.[29]

## III. RESULTS AND DISCUSSION

### A. Paramagnetic resonances

A comprehensive ESR study of the paramagnetic state above the phase transitions in $(TMTSF)_2PF_6$, $(TMTTF)_2PF_6$, $(TMTTF)_2ClO_4$, and $(TMTTF)_2Br$ was given by the authors elsewhere.[3] Here we confine ourselves in shortly presenting new results on $(TMTSF)_2AsF_6$ and compare them with the findings on the other compounds.

Above the phase transitions the TMTSF salts subject of the present study are quasi-one-dimensional metals. At room temperature we observe a conduction electron spin resonance signal near $g=2$ with a linewidth (HWHM) $\Delta H\approx200$ Oe. The $g$ value and the linewidth have a distinct anisotropy: they are both largest in the $c^*$ direction and smallest in the $a$ direction. In Fig. 1 the temperature dependences of the ESR intensity (area under absorption curve) which is proportional to the spin susceptibility $\chi_s$, the linewidth, and the $g$ shift $\Delta g=g-2.002319$ of $(TMTSF)_2AsF_6$ are displayed. Below room temperature the spin susceptibility and the linewidth decrease almost linearly down to 120 K. In the region between 120 K and $T_{SDW}=12$ K a smooth change in the slope of both quantities is observed: while the slope of $\chi_s$ decreases the slope of $\Delta H$ becomes larger as the temperature drops. As shown in Fig. 1(c), the $g$ shifts show only a very weak temperature dependence implying that the internal field is basically constant in the metallic phase. At $T_{SDW}$ the signal broadens and vanishes within a small temperature interval $\Delta T\approx1$ K. We also observe an increase of $g$ in $c^*$ direction and a decrease in $a$ and $b'$ direction indicating a rapid change of the local field. The results on $(TMTSF)_2PF_6$ are qualitatively and quantitatively similar.[3] In contrast, in the sulfur compounds $(TMTTF)_2X$ the ESR lines are fifty times smaller and the $g$ shifts are five times smaller than in $(TMTSF)_2X$ and above room temperature, the spin susceptibility exhibits a characteristic maximum.

Since the large thermal expansion along the organic stacks has visible effects on the temperature dependence of

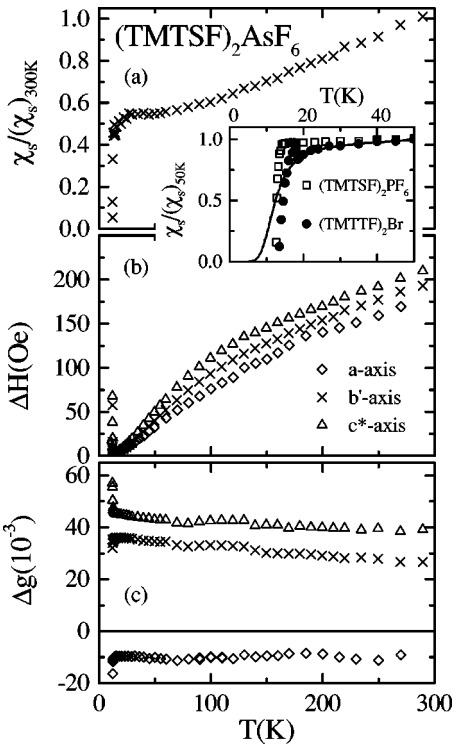


FIG. 1. Temperature dependence of (a) of the ESR intensity, (b) the linewidth $\Delta H$, and (c) the $\Delta g$ value of $(TMTSF)_2AsF_6$ in the three crystal directions as indicated. The inset shows an enlarged view of the spin susceptibility of $(TMTSF)_2PF_6$ and $(TMTTF)_2Br$ near the antiferromagnetic phase transition measured in the $b'$ direction.

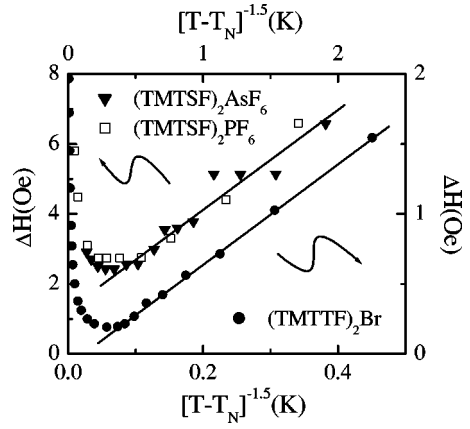


FIG. 2. Linewidth $\Delta H$ vs $(T-T_N)^{-1.5}$ of $(TMTSF)_2AsF_6$ and $(TMTSF)_2PF_6$ (left and top axes) and $(TMTTF)_2Br$ (right and bottom axes) above the antiferromagnetic phase transition in the $b'$ direction. $T_N=12$ K for the selenium compounds and $T_N=13.3$ K for $(TMTTF)_2Br$.

the spin susceptibility, we transformed the spin susceptibility at constant pressure $(\chi_s)_p$ into the spin susceptibility at constant volume $(\chi_s)_V$ using the scaling introduced by Wzietek *et al.* in case of $(TMTSF)_2PF_6$.[30] In $(TMTSF)_2AsF_6$ and $(TMTSF)_2PF_6$ the spin susceptibility at constant volume shows a weaker temperature dependence than seen for the spin susceptibility at constant pressure in Fig. 1(a). This behavior can be fitted satisfactorily in the framework of the Hubbard model in the limit of strong Coulomb repulsion. In both compounds exchange constant is given by $J=1400$ K. The $(TMTTF)_2X$ compounds can be described as $S=1/2$ antiferromagnetic Heisenberg chains with completely localized spins.[31] The exchange constants are smaller than in $(TMTSF)_2X$, in $(TMTTF)_2Br$ we derived $J=500$ K. Going from the insulating $(TMTTF)_2PF_6$ to the highly metallic $(TMTSF)_2AsF_6$ there is a sudden change in the charge-transport properties when the transfer integral in $b$ direction becomes comparable to the charge gap, while the spin dynamics changes continuously described by a steadily increasing exchange constant. We interpret this behavior as an indication of the separation of spin and charge degrees of freedom. As pointed out in detail in Ref. 3, spin-phonon coupling is the dominant relaxation process in the organic compounds investigated. The stronger spin-orbit coupling in selenium is responsible for the remarkable increase in $g$ shift and linewidth when going from $(TMTTF)_2X$ to $(TMTSF)_2X$. Additionally, we found out that the reduced linewidth $\Delta H_{red}=\Delta H/\Delta g^2$ increases linearly with the ratio $\gamma_C$ between twice the van der Waals radius of S or Se and the shortest interstack distances between the chalcogen atoms. We proved that $\Delta H_{red}$ is a measure of the interactions between the organic stacks in the $(TMTCF)_2X$ salts and gives a good estimate of the dimensionality.

The inset of Fig. 1 gives an enlarged view on the spin susceptibility of $(TMTSF)_2PF_6$ and $(TMTTF)_2Br$ in the vicinity of the antiferromagnetic phase transition. In $(TMTTF)_2Br$ $\chi_s$ slowly decreases for temperatures $T\leqslant 50$ K, at 19 K there is a sudden increase of the intensity before the ESR signal vanishes within a temperature range $\Delta T=4$ K. Between 19 and 50 K the spin susceptibility can be fitted using a model of one-dimensional lattice fluctuations[32] with a characteristic temperature $T_{SP}^0=50$ K which describes the behavior of a spin-Peierls system in the pseudo gap regime below $T_{SP}^0$. Such a decrease of $\chi_s$ was also observed in the spin-Peierls system $(TMTTF)_2PF_6$ with $T_{SP}^0=62$ K.[33,3] At $T=19$ K, a few degrees above the AFM phase transition, these lattice fluctuations collapse in $(TMTTF)_2Br$. No noticeable decrease of $\chi_s$ is observed above $T_{SDW}$ in $(TMTSF)_2AsF_6$ and $(TMTSF)_2PF_6$ which implies the absence of lattice fluctuations. Our findings are not in contradiction to x-ray diffusive scattering investigations[34] where below 175 K weak $2k_F$ CDW fluctuations were found. Since these one-dimensional lattice fluctuations extend over a large temperature range and are less critical than in $(TMTTF)_2Br$,[35] the spin susceptibility is not strongly affected by them.

### B. Antiferromagnetic fluctuations

The antiferromagnetic phase transition is accompanied by a strong increase of the linewidth in all crystal directions. In Fig. 1(b) this is shown for the example of $(TMTSF)_2AsF_6$; the same behavior is observed in $(TMTSF)_2PF_6$ and $(TMTTF)_2Br$. A detailed analysis of the temperature dependence of the linewidth $\Delta H$ of all materials investigated near the antiferromagnetic phase transitions is given in Fig. 2. A linear increase of the linewidth is observed in this representation $\Delta H$ vs $(T-T_N)^{-1.5}$ in all three organic systems, i.e., the linewidth follows a critical behavior $\Delta H\propto[(T$

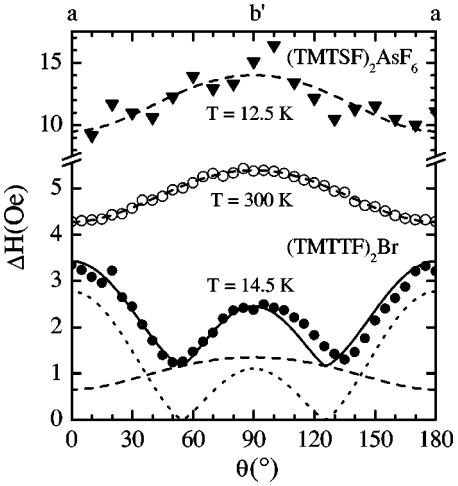


FIG. 3. Angular dependence of the linewidth $\Delta H$ of $(TMTSF)_2AsF_6$ and $(TMTTF)_2Br$ in the regime of antiferromagnetic fluctuations (closed symbols) and of $(TMTTF)_2Br$ at $T=300$ K (open circles). The dashed lines represent fits with $\Delta H=[\Delta H_a^2\cos^2(\theta)+\Delta H_{b'}^2\sin^2(\theta)]^{1/2}$ (spin-phonon interaction), the dotted line a fit with $H_{dd}=\Delta H_{b'}[3\cos^2(\theta)-1]^{4/3}$ (dipole-dipole interaction), and the solid line is the sum of both.

$-T_N)/T_N]^{-\mu}$. In the case of dipole-dipole interaction the exponent $\mu$ is given by $\mu=3-d/2$, i.e., $\mu=1.5$ for three-dimensional ($d=3$) antiferromagnetic fluctuations. These results are confirmed by NMR investigations where a critical behavior in the relaxation rate $1/T_1$ was observed in $(TMTSF)_2PF_6$ (Ref. 36) and $(TMTTF)_2Br$.[37]

At room temperature the angular dependence of $g$ value and linewidth $\Delta H$ is the same for the selenium and sulfur compounds. Measuring in the $a$-$b'$ plane the angular dependence is given by $\Delta H=\sqrt{\Delta H_a^2\cos^2(\theta)+\Delta H_{b'}^2\sin^2(\theta)}$ as seen in Fig. 3 (open circles). Spin-phonon interaction is the main relaxation process well above the phase transitions. The solid symbols in Fig. 3 show the angular dependence of the linewidth of $(TMTSF)_2AsF_6$ and $(TMTTF)_2Br$ in the regime of antiferromagnetic fluctuations. Apart from scatterings due to thermal instabilities the angular dependence of $\Delta H$ remains unchanged in $(TMTSF)_2AsF_6$. In contrast, the behavior in $(TMTTF)_2Br$ is completely different. Rotating the sample in the $a$-$b'$ plane, the broadest ESR line is measured in $a$ direction ($\theta=0°$) and the smallest lines at $\theta=55°$ in the $a$-$b'$ plane. Along the $b'$ axis ($\theta=90°$) the linewidth has an intermediate value. The minimum near the magic angle $\theta=54.7°$ is a strong indication for dipole-dipole interaction. In the case that dipole interaction is the dominant relaxation process in one-dimensional systems, an angular dependence $\Delta H_{dd}=\Delta H_{b'}(3\cos^2\theta-1)^{4/3}$ is expected. As seen in the lower part of Fig. 3 the orientation dependent measurements of the linewidth of $(TMTTF)_2Br$ at $T=14.5$ K can be fitted with the sum of the contributions of the dipole-dipole and spin-phonon interaction. The spin-phonon interaction becomes less prominent with decreasing temperature; the spin-orbit coupling constant $\lambda$ in sulfur is approximately five times weaker than in selenium. This lowers the spin-orbit contribution to the linewidth of $(TMTTF)_2X$ by a factor of 25 (Ref. 38) while the dipole-dipole interaction increases strongly in the vicinity of the antiferromagnetic phase transition. Our findings are in good agreement with the fact that the spin-orbit contributions cannot be neglected in the antiferromagnetic ground state of the selenium compounds. The existence of a finite spin-phonon interaction is responsible for the interchange of the magnetic intermediate and hard axis. The spin-orbit anisotropy favors the $a$ direction and therefore in $(TMTSF)_2X$ the hard axis is changed to the intermediate axis.[38]

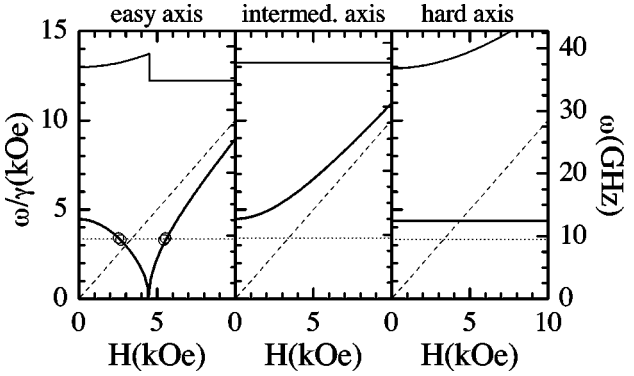


FIG. 4. Frequency dependence of the AFMR-fields in the three crystal directions. The solid lines represent the theoretical predictions for $(TMTSF)_2PF_6$ using $\Omega_-=12.5$ GHz and $\Omega_+=36.9$ GHz (see Table I) considering the anisotropy of the $g$ values. The open circles denote the experimental data at $T=4.2$ K for $\nu=9.12$ GHz and $\nu=9.48$ GHz. Additionally the $X$-band frequency (dotted lines) and the position of the electron paramagnetic resonance (dashed lines) are shown.

### C. Antiferromagnetic resonances

While conduction electron spin resonance excites single spin flips, antiferromagnetic resonances probe the absorption due to the collective mode of the ordered spin system. At the beginning of the fifties, Kittel[39] and Nagamiya[40] developed the theory of antiferromagnetic resonances for uniaxial antiferromagnets. Later, the theory was extended to the case of orthorhombic anisotropy by Yosida,[41] Ubbink,[42] and Nagamiya.[43] The organic linear chain compounds investigated in this work have a triclinic crystal structure. Such systems are characterized by the most general form of magnetic anisotropy, so we have to apply the AFMR theory for orthorhombic anisotropy. This anisotropy can be described using the zero-field modes[27]

$$\Omega_+(H=0)=\frac{\mu}{\mu_B}\gamma_e\sqrt{J(D+E)},$$

$$\Omega_-(H=0)=\frac{\mu}{\mu_B}\gamma_e\sqrt{2JE} \qquad (1)$$

with $J$ the exchange parameter, $D>E$ are the two anisotropy parameters, $\mu$ the magnitude of the local magnetic moment, $\mu_B$ the Bohr magneton, and $\gamma_e$ the electronic gyromagnetic ratio. The field dependence of the modes along the magnetic easy, intermediate, and hard axis is depicted in Fig. 4 for $(TMTSF)_2AsF_6$. Since the materials were investigated at $X$-band frequency $\nu\approx9.5$ GHz it was only possible to excite the low-frequency modes along the easy and intermediate axis. Along the easy axis, at finite temperature for $D,E\ll J$ and $H\ll J$ the field dependence is given by

$$\nu(H)=\frac{1}{\sqrt{2}}\sqrt{(1+\alpha^2)H^2\gamma_i^2+\Omega_-^2+\Omega_+^2\pm\sqrt{(1+\alpha^2)^2H^4\gamma_i^4+2(1+\alpha)^2H^2\gamma_i^2(\Omega_-^2+\Omega_+^2)+(\Omega_-^2-\Omega_+^2)^2}} \quad (2)$$

for the $\Omega_-$ mode ($H<H_{sf}$) and

$$\nu(H)=\sqrt{H^2\gamma_i^2-\Omega_-^2} \quad (3)$$

for the spin-flop mode ($H>H_{sf}$). Along the intermediate axis one obtains

$$\nu(H)=\sqrt{H^2\gamma_i^2+\Omega_-^2}. \quad (4)$$

$H_{sf}=\Omega_-/(\gamma_e\sqrt{\alpha})$ denotes the spin-flop field, $\alpha=1-\chi_\parallel/\chi_\perp$ is a measure of the susceptibility anisotropy below the antiferromagnetic phase transition, and $\gamma_i=\gamma_e g_i/2.00232$ ($i=a$, $b'$, or $c^*$) considers the anisotropy of the $g$ value as obtained from the paramagnetic resonance measurements along the $a$, $b'$, and $c^*$ axes above the phase transitions. If the anisotropy energy is only due to dipole-dipole interaction, the sublattice magnetization $M(T)$ and therefore the order parameter is proportional to $\Omega_-(T)$.[44] In this case the temperature dependence of the sublattice magnetization can be determined from the temperature dependence of the AFMR frequency using Eqs. (2), (3), or (4) for the individual modes.

If the field is not applied along the three magnetic axes, the AFMR fields are always a function of $\Omega_-$, $\Omega_+$, and $\nu$. The behavior gets rather complicated when the magnetic field $\vec{H}$ and common direction of the antiferromagnetic moments $\vec{M}'$ are not perpendicular, i.e., when the magnetic field is applied in the easy-intermediate plane or when the field is smaller than the spin-flop field and applied in the easy-hard plane. In consequence of this, the angle between $\vec{H}$ and $\vec{M}'$ is a function of the strength of the applied field and at finite temperatures the susceptibility anisotropy parameter $\alpha$ has to be considered. The complex formulas for the field and angular dependences of the modes in the different crystal plains were given by Nagamiya in Ref. 43.

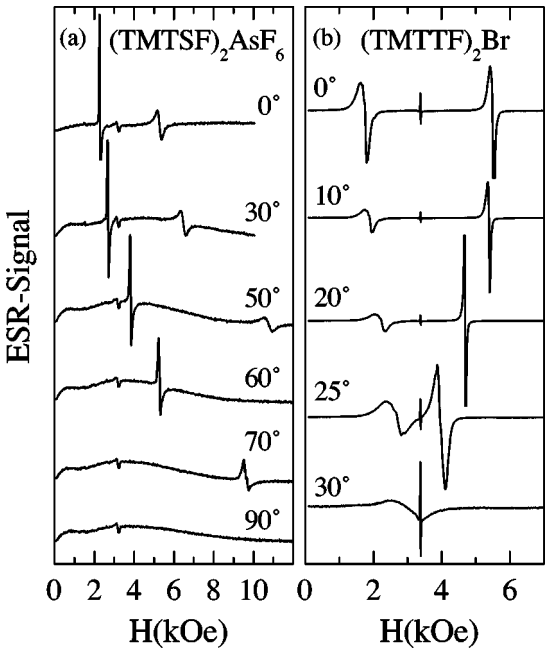


FIG. 5. AFMR spectra of $(TMTSF)_2AsF_6$ (a) and $(TMTTF)_2Br$ (b) in the $b'$-$c^*$ plane at $T=4.2$ K for different orientations ($0°\equiv b'$ direction).

### *1. SDW ground state in $(TMTSF)_2X$*

In the spin-density-wave ground state, the Bechgaard salts $(TMTSF)_2AsF_6$ and $(TMTSF)_2PF_6$ show the behavior of the static susceptibility typically expected for an antiferromagnet.[12] Along the $b'$ direction, $\chi(T)$ drops rapidly indicating the easy axis; the hard and intermediate axes are oriented in the $c^*$ and $a$ direction, respectively. The spin susceptibility obtained from the ESR intensity is in general isotropic since it does not measure a microscopic magnetization. Antiferromagnetic fluctuations give rise to a dramatic broadening of the paramagnetic resonance line in the vicinity of the phase transition at $T_{SDW}\approx 12$ K. Additionally, due to the development of internal magnetic fields associated with

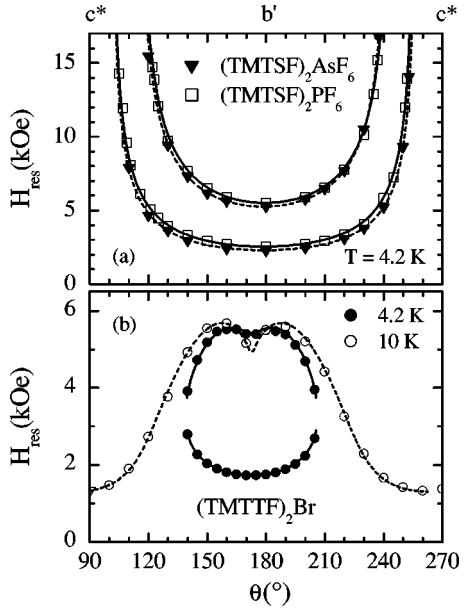


FIG. 6. Angular dependence of the AFMR field $H_{res}$ observed in the $b'$-$c^*$ plane of the materials investigated. The lines were calculated using the equations derived by Nagamiya (Ref. 43). The upper panel (a) shows the low-field and high-field resonances of $(TMTSF)_2AsF_6$ and $(TMTSF)_2PF_6$ at $T=4.2$ K. For $(TMTSF)_2AsF_6$ we obtained the zero-field modes $\Omega_-=11.5$ GHz and $\Omega_+=34.1$ GHz (dashed lines) and for $(TMTSF)_2PF_6$ $\Omega_-=12.2$ GHz and $\Omega_+=36.5$ GHz (solid lines). In the lower panel (b) the angular dependence of $H_{res}$ of $(TMTTF)_2Br$ is shown. At $T=4.2$ K the data (closed circles) can be well described with $\Omega_-=11.8$ GHz, $\Omega_+=19.4$ GHz, and $\alpha=0.88$ (solid lines) and at $T=10$ K (open circles) with $\Omega_-=8.8$ GHz, $\Omega_+=14.7$ GHz, and $\alpha=0.44$ (dashed line).

the appearance of a magnetic moment on the TMTSF molecules the resonances are shifted in field. The signal fully vanishes within a temperature interval of 1 K in all three directions. All the charge carriers and thus all the spins enter a collective state, in which the spins form pairs; this behavior is evidence for the development of a spin-density wave.

Well below the SDW phase transition, at $T=4.2$ K the ESR-spectra shown in Fig. 5(a) for $(TMTSF)_2AsF_6$ were recorded. Along the $b'$ direction two resonances are observed,[45] one at $H_{res_1}\approx 2300$ Oe and the other at $H_{res_2}\approx 5300$ Oe. While rotating the samples around the $a$ axis, the resonances are shifted towards higher fields. With increasing angle $\theta$ the signals broaden and the amplitudes decrease. Along the $c^*$ axis no resonance is observed. This pattern is typical for antiferromagnetic resonance measurements when the plane includes the easy and hard axis. The first resonance can be attributed to the $\Omega_-$ mode and the second to the spin-flop mode. The intensity of the antiferromagnetic resonance signals is of the same order of magnitude as the intensity of the paramagnetic resonance just above the transition.

The angular dependences of the antiferromagnetic resonance fields determined from the spectra shown in Fig. 5(a) are plotted in Fig. 6(a). For both materials, they show the same behavior as expected in the theory of AFMR for a antiferromagnet with orthorhombic symmetry in the plane with the magnetic easy and hard axis. Using the same parameters, the $\Omega_-$ as well as the spin-flop mode can be well described by the equations derived by Nagamiya.[43] At 4.2 K we obtained $\Omega_-=11.5$ GHz and $\Omega_+=34.1$ GHz for $(TMTSF)_2AsF_6$ and $\Omega_-=12.2$ GHz and $\Omega_+=36.2$ GHz for $(TMTSF)_2PF_6$. Additionally, the $\Omega_-$ mode yields $\alpha=0.9$ for both compounds.

By increasing the temperature from $T=4.2$ K the resonance fields are shifted towards lower fields as shown in Fig. 7(a) because the internal magnetic fields get weaker. Consequently, the zero field modes and therefore the AFMR fields along $b'$ direction should decrease. Below 4.2 K the AFMR fields are only weakly temperature dependent. The shift towards lower fields in $H_{res_1}$ and higher fields in $H_{res_2}$ is due to the different microwave-resonance frequency of the cylindrical cavity used for the bath cryostat measurements at $T\leqslant 4.2$ K. From the temperature dependence of the resonance fields the temperature dependence of the zero-field mode $\Omega_-$ can be calculated using Eq. 2 and the static susceptibility measurements of Mortensen *et al.*[12] In Fig. 8(a) the temperature dependence of $\Omega_-$ is plotted together with the reduced local field determined from NMR and $\mu$SR measurements on $(TMTSF)_2PF_6$ by Takahashi *et al.*[18] and Le *et al.*[9] The temperature dependence of the local field can be seen as a measure of the order parameter of the SDW ground state. There are clear deviations from the behavior predicted by the mean-field theory. As already pointed out by Clark *et al.*[7] the order parameter increases rapidly just below $T_{SDW}$. This may imply that the SDW transition in these quasi one-dimensional systems is not simply a second-order phase transition but shows a tendency via first order.

From the temperature dependence of $\Omega_-$ and $\Omega_+$ the frequencies of the zero-field modes at $T=0$ K and therefore the spin-flop fields can be extrapolated. We obtain $\Omega_-=11.7$ GHz, $\Omega_-=34.6$ GHz, and $H_{sf}=4.2$ kOe for $(TMTSF)_2AsF_6$ and $\Omega_-=12.5$ GHz, $\Omega_-=36.9$ GHz, and $H_{sf}=4.5$ kOe for $(TMTSF)_2PF_6$, respectively. As summarized in Table I, the

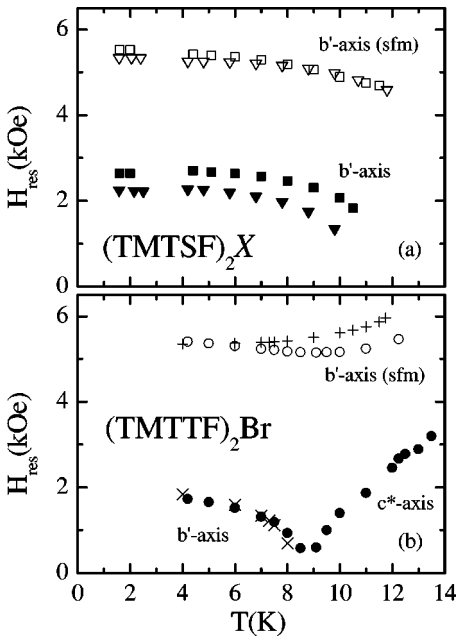


FIG. 7. (a) Temperature dependence of the resonance fields of the low-frequency (closed symbols) and spin-flop mode (open symbols) of $(TMTSF)_2AsF_6$ ($\nabla$) and $(TMTSF)_2PF_6$ ($\square$) in $b'$ direction. (b) Temperature dependence of the resonance fields of the low-frequency mode in $b'$ and $c^*$ direction ($\bullet$) and the spin-flop mode in $b'$ direction ($\circ$) of $(TMTTF)_2Br$. Additionally, the low-frequency ($\times$) and spin-flop mode ($+$) determined from the measurements in the $a$-$b'$ plane are plotted.

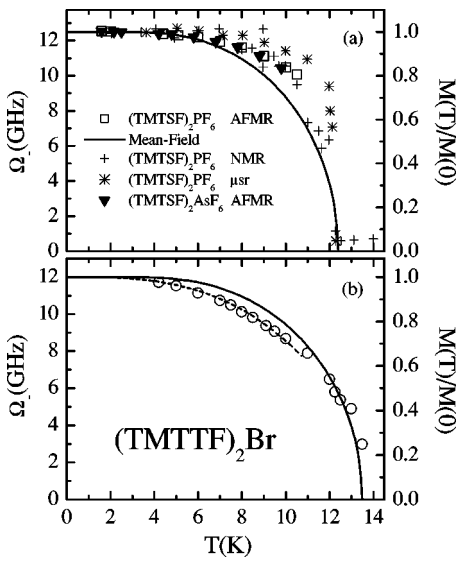


FIG. 8. (a) Temperature dependence of the low-frequency zero-field mode $\Omega_-$ of $(TMTSF)_2PF_6$. The results are compared with the predictions of the mean-field theory, NMR-measurements of Takahashi *et al.* (Ref. 18), $\mu$SR-measurements of Le *et al.* (Ref. 9), and the temperature dependence of $\Omega_-/\Omega_-(0)$ of $(TMTSF)_2AsF_6$. (b) Temperature dependence of $\Omega_-$ of $(TMTTF)_2Br$. The solid line represents the temperature dependence of the sublattice magnetization expected in mean-field theory, the dashed line corresponds to $M(T)/M(0)=1-cT^3$ with $c=2.7\times 10^{-4}$ K$^{-3}$.

values for $(TMTSF)_2AsF_6$ are somewhat smaller than the findings of Torrance *et al.* at *Q*-band frequencies;[16] no data on $(TMTSF)_2PF_6$ have yet been published. Together with the exchange constant $J$ which was derived from temperature dependence of the spin susceptibility in the paramagnetic state and the amplitude of the spin-density-waves $\mu/\mu_B = 0.08$ for both materials[18] the anisotropy energies $D$ and $E$ can be determined using Eq. (1). We obtain $D = 0.29$ K and $E = 0.018$ K in $(TMTSF)_2AsF_6$ and $D = 0.33$ K and $E = 0.02$ K in $(TMTSF)_2PF_6$, respectively. The square-frequency ratio $(\Omega_+/\Omega_-)^2 = (D+E)/(2E) = 8.7 \gg 1$ is the same in both compounds indicating that they are near to the limit of an easy plane antiferromagnet with a small inplane anisotropy.

#### 2. *Antiferromagnetic ground state in* $(TMTTF)_2Br$

In contrast to the spin-density-wave ground state, in $(TMTTF)_2Br$ the antiferromagnetic phase transition is induced by a three-dimensional ordering of the quasi one-dimensional chains of localized spins. A finite interchain coupling which is characterized by the exchange constant $J_\perp$ gives rise to the phase transition. Following Ogushi,[46] from the transition temperature $T_N = 13.3$ K and $J = 500$ K the ratio between the interchain and intrachain coupling can be estimated with $J_\perp/J \approx 0.001$, i.e., $J_\perp \approx 0.5$ K. As discussed in detail in Sec. III B the magnetic anisotropy of the antiferromagnetic ground state of the sulfur compounds differs from that of the selenium compounds: the hard axis is orientated along the $a$ direction and the intermediate axis along the $c^*$ direction, while the easy axis is as well orientated in the $b'$ direction. The change in the anisotropy is explained by stronger effects of the spin-orbit coupling in $(TMTSF)_2X$ which favor the $a$ direction.

Upon cooling the sample, the paramagnetic resonance observed in the high-temperature range vanishes almost completely at the AFM phase transition within a temperature interval of 4 K in all three crystal directions. The absorption spectra of $(TMTTF)_2Br$ recorded in the $b'$-$c$ plane at helium temperature are shown in Fig. 5(b). Along the $b'$ axis we observe two broad resonances similar to the selenium compounds. When the single crystal is rotated around the $a$ direction the two resonances converge before they are merging at $\theta = 30°$; for $\theta > 30°$ both lines vanish. Additionally, we observe a small line around $g \approx 2$. This line is much smaller and higher in amplitude than the signal observed in the TMTSF salts at nearly the same position. The anisotropy of this signal is the same as observed in the paramagnetic resonance above the AFM phase transition and the order of magnitude is similar to that of the signal observed in the spin-Peierls compound $(TMTTF)_2PF_6$ well below $T_{SP}$ at $T = 4.2$ K.[3] Therefore this resonance can be attributed to paramagnetic centers in the molecular stacks, for example the ends of spin chains which are not covered by the antiferromagnetic ordering. Since the spin-density-wave ground state of the selenium compounds is incommensurable to the crystal structure this feature is only observed in the sulfur compound with a commensurable antiferromagnetic ground state. It would be interesting to see if by applying pressure the additional signal vanishes at around $p = 5$ kbar where a transition from the commensurate to an incommensurate AFM ground state is expected in $(TMTTF)_2Br$.[47]

In Fig. 6(b) the angular dependence of the antiferromagnetic resonances in $(TMTTF)_2Br$ is plotted for $T = 4.2$ K and $T = 10$ K. At both temperatures the observed patterns are completely different to those in $(TMTSF)_2X$ which is due to the change in anisotropy. Indeed, when a AFMR measurement is carried out in the $a$-$b'$ plane of the bromide compound (not shown) we observe the same angular dependence as displayed in the upper part of Fig. 6 for $(TMTSF)_2AsF_6$ in the $b'$-$c^*$ plane. The rotation bubble at $T = 4.2$ K shown in Fig. 6(b) is characteristic for a measurement in the plane including the easy and intermediate axis.[26] We determined a shift $\theta_0 = -7°$ between the magnetic axes and the crystallographic axes. The resonance fields along the easy axis are given by $H_{res_1}(\theta_0) = 1730$ Oe and $H_{res_2}(\theta_0) = 5380$ Oe. To understand the angular dependence at 10 K it is necessary to look at the temperature dependence of the AFMR fields displayed in Fig. 7(b). With increasing temperature well below $T_N$ $H_{res_2}$ is nearly temperature independent while $H_{res_1}$ decreases. At $T = 8.8$ K the low-field resonance vanishes completely. By further increasing the temperature a new resonance appears along the $c^*$ direction (intermediate axis). This behavior can be explained by the decrease of $\Omega_-$ with rising temperature. According to Eq. (2) the low-field resonance along the easy axis should vanish for $\nu = \Omega_-$. In $(TMTTF)_2Br$ this point is reached at $T = 8.8$ K. Above this characteristic temperature, $\Omega_-$ falls below $\nu$ and we observe a new antiferromagnetic resonance along the intermediate axis which is shifted towards higher fields by further increasing temperature. At $T = 10$ K we observe one resonance in $b'$ and one in $c^*$ direction, respectively, as seen in Fig. 6(b). At both temperatures, the angular dependence of the AFMR can be well fitted with the equations given by Nagamiya.[43] The low-frequency zero-field mode $\Omega_-$ decreases from 11.8 GHz at 4.2 K to 8.8 GHz at 10 K, the high-frequency zero-field mode $\Omega_+$ from 19.4 to 14.7 GHz, and the susceptibility-anisotropy parameter $\alpha$ from 0.88 to 0.43. There is a good agreement between $\alpha$ determined from the angular dependent AFMR measurements and the static susceptibility measurements performed by Parkin *et al.*[26] It is remarkable that the parallel susceptibility $\chi_\parallel$ decreases much slower in $(TMTTF)_2Br$ than in the selenium compounds below the AFM phase transition.

Again, we derived the temperature dependence of $\Omega_-$ from the temperature dependences of the resonance fields using Eqs. (2) and (4). Since the spin-orbit contributions to the anisotropy energies in the sulfur compounds are very small, $\Omega_-$ is directly proportional to the sublattice magnetization $M$.[44] Hence, $\Omega_-(T)$ should follow the temperature dependence of the order parameter. Figure 8(b) shows the temperature dependence of $\Omega_-$. Unlike the observations in $(TMTSF)_2X$, even at low temperatures $\Omega_-$ has a distinct temperature dependence which is much stronger as expected for the order parameter of a $S = 1/2$ antiferromagnet in mean-field theory [solid line in Fig. 8(b)]. Such a behavior is a strong indication for the appearance of thermal magnons in the low-temperature regime. In magnetically ordered materials such as ferromagnets or antiferromagnets, the sublattice magnetization can be lowered by the excitation of thermal magnons. For a two-sublattice antiferromagnet the deviation

of the magnetization can be calculated in the framework of the spin-wave theory. Since the anisotropy energies in the materials investigated are very small (see Table I) we can assume a linear dispersion relation $\omega \propto q$ for the magnons. If $M(0)$ is the magnetization in the absence of magnons, at low temperatures $T \ll T_N$ the deviation of the magnetization $M(0)-M(T)$ caused by the thermal magnons is proportional to $(T/J)^3$, the same temperature dependence is found in other thermodynamic quantities such as specific heat and entropy.[48] The dashed line in Fig. 8(b) represents a fit which considers the spin wave contributions using $\Omega_-(0)=12$ GHz or $M(0)=4.282$ kG, respectively. Below $T=10$ K the data are well fitted by the model. Near the AFM phase transition higher terms in the magnon-dispersion relation have to be considered and fluctuation effects may influence the data, additionally. In the $(TMTSF)_2$ salts the effects of thermal magnons can be neglected since the weakening of the sublattice magnetization is proportional to $J^{-3}$ and the exchange constant is nearly three times larger than in $(TMTTF)_2Br$. Thus, it is not surprising that we found no contributions of spin waves in the experiments on $(TMTSF)_2PF_6$ and $(TMTSF)_2AsF_6$.

Our new results on $(TMTSF)_2PF_6$ agree very well with other experiments probing the internal field such as NMR (Ref. 18) and $\mu$SR,[9] but also acoustic investigations[19] and measurements of the energy gap by optical[6] and transport methods.[5] In this regard, it would be of interest to study the magnetic structure and the order parameter of field induced spin-density waves as found in $(TMTSF)_2PF_6$ and $(TMTSF)_2ClO_4$. These investigations, however, can only be carried out by neutron scattering methods, experiments which have not been done yet.

## IV. CONCLUSION

The results determined by our paramagnetic and antiferromagnetic resonance studies on $(TMTSF)_2PF_6$, $(TMTSF)_2AsF_6$, and $(TMTTF)_2Br$ presented in this work are listed in Table I together with results from other groups. In all compounds, the zero-field mode $\Omega_-$ at $T=0$ K, the spin-flop field $H_{sf}$, and the anisotropy energy $E$ are nearly the same while $\Omega_+$ and therefore the anisotropy energy $D$ are much higher in $(TMTSF)_2X$ than in $(TMTTF)_2X$. In the (TMTTF) salts, just as in the (TMTSF) compounds, the ratio $(\Omega_+/\Omega_-)^2=(D+E)/(2E)\approx 2.8$ is independent from the anion $X$. Consequently, the anisotropy of the antiferromagnetic ground state is determined by the weight of the spin-orbit coupling in relation to the dipole-dipole interaction, i.e. by the spin-orbit coupling constant of the chalcogen atoms. The influence of the coupling of the spin-density wave to the lattice is discussed in several recent publications.[6,19] If the ground state of $(TMTSF)_2PF_6$ is a mixture between a SDW and a CDW as suggested by x-ray investigations[20] the SDW can be collectively depinned by applying an electric field which exceeds the threshold field of the nonlinear conductivity.[5,7,4] We expect that the AFMR disappear and the original paramagnetic-resonance signal reappears. These experiments are in progress.

We found distinct differences in temperature dependence of the order parameter of the selenium and the sulfur salts. In the former the findings of NMR and $\mu$SR investigations on $(TMTSF)_2PF_6$ which reveal a tendency towards first-order phase transitions are confirmed by this work. The same behavior is observed when the anion $PF_6$ is replaced by $AsF_6$. We showed that the sublattice magnetization of $(TMTTF)_2Br$ has a much stronger temperature dependence at low temperatures. This can be explained by the excitation of thermal magnons which reduce the magnetization expected from mean-field theory.

In the paramagnetic state the temperature dependence of the spin susceptibility can be described within the framework of the Hubbard model in the limit of strong Coulomb repulsion. The ESR linewidth $\Delta H$ is dominated by spin-phonon interaction. In the vicinity of the phase transitions we find evidence of antiferromagnetic fluctuations in $(TMTTF)_2Br$, $(TMTSF)_2PF_6$, and $(TMTSF)_2AsF_6$ which follow the critical behavior $\Delta H \propto [(T-T_N)/T_N]^{-1.5}$ expected for three-dimensional ordering.

## ACKNOWLEDGMENTS

The work at Augsburg was supported by the BMBF under Contract No. EKM 13N6917. The crystal growth at UCLA was supported by the National Science Foundation. The work at Bloomington was supported by the Division of Material Research of the National Science Foundation (Grant No. DMR-9414268).

*Present address: Department of Physics, University of California at San Diego, La Jolla, CA 92093-0319. Email address: mdumm@physics.ucsd.edu

[1] D. Jérome and H. J. Schulz, Adv. Phys. **31**, 299 (1982).

[2] C. Bourbonnais and D. Jérome, in *Advances in Synthetic Metals*, edited by P. Bernier, S. Lefrant, and G. Bidan (Elsevier, Amsterdam, 1999); C. Bourbonnais and D. Jérome, Science **281**, 1155 (1998).

[3] M. Dumm, A. Loidl, B. W. Fravel, K. P. Starkey, L. K. Montgomery, and M. Dressel, Phys. Rev. B **61**, 511 (2000).

[4] G. Grüner, Rev. Mod. Phys. **66**, 1 (1994).

[5] G. Mihály, Y. Kim, and G. Grüner, Phys. Rev. Lett. **67**, 2713 (1991); **66**, 2806 (1991); O. Traetteberg, G. Kriza, and G. Mihály, Phys. Rev. B **45**, 8795 (1992); F. Zámborszky, G. Szeghy, G. Abdussalam, L. Forró and G. Mihály, *ibid.* **60**, 4414 (1999).

[6] L. Degiorgi, M. Dressel, A. Schwartz, B. Alavi, and G. Grüner, Phys. Rev. Lett. **76**, 3838 (1996); M. Dressel, L. Degiorgi, J. Brinkmann, A. Schwartz, and G. Grüner, Physica B **230-232**, 1008 (1997); V. Vescoli, L. Degiorgi, M. Dressel, A. Schwartz, W. Henderson, B. Alavi, G. Grüner, J. Brinkmann, and A. Virosztek, Phys. Rev. B **60**, 8019 (1999).

[7] W. G. Clark, M. E. Hanson, W. H. Wong, and B. Alavi, J. Phys. IV **3**, 235 (1993); Physica B **194-196**, 285 (1994); W. H. Wong, M. E. Hanson, B. Alavi, W. G. Clark, and W. A. Hines, Phys. Rev. Lett. **70**, 1882 (1993); W. H. Wong, M. E. Hanson, W. G. Clark, B. Alavi, and G. Grüner, *ibid.* **72**, 2640 (1994).

[8] Earlier NMR work has been performed by Andrieux *et al.* [J. Phys. (France) Lett. **42**, L87 (1981)] and Scott *et al.* [Phys. Rev. B **24**, 475 (1981)].

[9] L. P. Le, A. Keren, G. M. Luke, B. J. Sternlieb, W. D. Wu, Y. J.

Uemura, J. H. Brewer, T. M. Riseman, R. V. Upasani, L. Y. Chiang, W. Kang, P. M. Chaikin, T. Csiba, and G. Grüner, Phys. Rev. B **48**, 7284 (1993).
[10] K. Bechgaard, C. S. Jacobsen, K. Mortensen, H. J. Pedersen, and N. Thorup, Solid State Commun. **33**, 1119 (1980).
[11] J. C. Scott, H. J. Pedersen, and K. Bechgaard, Phys. Rev. Lett. **45**, 2125 (1980); Phys. Rev. B **24**, 475 (1981).
[12] K. Mortensen, Y. Tomkiewicz, T. D. Schultz, and E. M. Engler, Phys. Rev. Lett. **46**, 1234 (1981); K. Mortensen, Y. Tomkiewicz, and K. Bechgaard, Phys. Rev. B **25**, 3319 (1982).
[13] H. J. Pedersen, J. C. Scott, and K. Bechgaard, Solid State Commun. **35**, 207 (1980); H. J. Pedersen, J. C. Scott, and K. Bechgaard, Phys. Rev. B **24**, 5014 (1981).
[14] J. C. Scott, Mol. Cryst. Liq. Cryst. **79**, 49 (1982).
[15] S. Flandrois, C. Coulon, P. Delhaes, D. Chasseau, C. Hauw, J. Gaultier, J. M. Fabre, and L. Giral, Mol. Cryst. Liq. Cryst. **79**, 307 (1982).
[16] J. B. Torrance, H. J. Pedersen, and K. Bechgaard, Phys. Rev. Lett. **49**, 881 (1982).
[17] W. M. Walsh, F. Wudl, E. Aharon-Shalom, L.W. Rupp, J.M. Vandenberg, K. Andres, and J. B. Torrance, Phys. Rev. Lett. **49**, 885 (1982).
[18] T. Takahashi, Y. Maniwa, H. Kawamura, and G. Saito, J. Phys. Soc. Jpn. **55**, 1364 (1986).
[19] S. Zherlitsyn, G. Bruls, A. Goltsev, B. Alavi, and M. Dressel, Phys. Rev. B **59**, 13 861 (1999); M. Dressel, Physica C **317-318**, 89 (1999).
[20] J. P. Pouget and S. Ravy, J. Phys. I **6**, 1501 (1996).
[21] M. Dressel, A. Schwartz, G. Grüner, and L. Degiorgi, Phys. Rev. Lett. **77**, 398 (1996); J. Moser, M. Gabay, P. Auban-Senzier, D. Jérome, K. Bechgaard, and J. M. Fabre, Eur. Phys. J. B **1**, 39 (1998); A. Schwartz, M. Dressel, G. Grüner, V. Vescoli, L. Degiorgi, and T. Giamarchi, Phys. Rev. B **58**, 1261 (1998); V. Vescoli, L. Degiorgi, W. Henderson, G. Grüner, K. P. Starkey, and L. K. Montgomery, Science **281**, 1181 (1998).
[22] G. Mihály, I. Krézsmárki, F. Zámborszky, and L. Forró, Phys. Rev. Lett. **84**, 2670 (2000); J. Moser, J. R. Cooper, D. Jérome, B. Alavi, S. E. Brown, and K. Bechgaard, *ibid.* **84**, 2674 (2000).
[23] T. Nakamura, T. Nobutoki, Y. Kobayashi, T. Takahashi, and G. Saito, Synth. Met. **70**, 1293 (1995).
[24] T. Nakamura, R. Kinami, T. Takahashi, and G. Saito, Synth. Met. **86**, 2053 (1997).
[25] P. Delhaes, C. Coulon, J. Amiell, S. Flandrois, E. Toreilles, J. M. Fabre, and L. Giral, Mol. Cryst. Liq. Cryst. **50**, 43 (1979).
[26] S. S. P. Parkin, J. C. Scott, J. B. Torrance, and E. M. Engler, Phys. Rev. B **26**, 6319 (1982); S. S. P. Parkin, J. C. Scott, J. B. Torrance, and E. M. Engler, J. Phys. (Paris), Colloq. **44**, C3-1111 (1983).
[27] C. Coulon, J. C. Scott, and R. Laversanne, Phys. Rev. B **33**, 6235 (1986).
[28] L. K. Montgomery, in *Organic Conductors*, edited by J. P. Farges (Marcel Dekker, New York, 1994), p. 138ff.
[29] The TMT*C*F salts have a triclinic crystal structure; nevertheless the angles are close to 90°. The $b'$ direction is normal to the $a$ axis, $c^*$ is normal to the $a$-$b'$ plane.
[30] P. Wzietek, F. Creuzet, C. Bourbonnais, D. Jérome, K. Bechgaard, and P. Batail, J. Phys. I **3**, 171 (1993).
[31] J. C. Bonner and M. E. Fisher, Phys. Rev. **135**, A640 (1964); S. Eggert, I. Affleck, and M. Takahashi, Phys. Rev. Lett. **73**, 332 (1994).
[32] C. Bourbonnais and B. Dumoulin, J. Phys. I **6**, 1727 (1996).
[33] F. Creuzet, C. Bourbonnais, L. G. Caron, D. Jérome, and K. Bechgaard, Synth. Met. **19**, 289 (1987).
[34] M. Ribault, J. P. Pouget, D. Jérome, and K. Bechgaard, J. Phys. (France) Lett. **41**, L607 (1980); J. P. Pouget, R. Moret, R. Comes, K. Bechgaard, J. M. Fabre, and L. Giral, Mol. Cryst. Liq. Cryst. **79**, 129 (1982).
[35] J. P. Pouget and S. Ravy, Synth. Met. **85**, 1523 (1997).
[36] C. Bourbonnais, P. Stein, D. Jérome, and A. Moradpour, Phys. Rev. B **33**, 7608 (1986).
[37] P. Wzietek, C. Bourbonnais, F. Creuzet, D. Jérome, and K. Bechgaard, Europhys. Lett. **12**, 453 (1990).
[38] M. Roger, J. M. Delrieu, and E. Wope Mbougue, Phys. Rev. B **34**, 4952 (1986).
[39] C. Kittel, Phys. Rev. **82**, 565 (1951); F. Keffer and C. Kittel, *ibid.* **85**, 329 (1952).
[40] T. Nagamiya, Prog. Theor. Phys. **6**, 350 (1951).
[41] K. Yosida, Prog. Theor. Phys. **7**, 425 (1952).
[42] J. Ubbink, Physica (Amsterdam) **19**, 919 (1953).
[43] T. Nagamiya, Prog. Theor. Phys. **11**, 309 (1954); T. Nagamiya, K. Yosida, and R. Kubo, Adv. Phys. **4**, 1 (1955).
[44] S. Foner, in *Magnetism*, edited by G.T. Rado and H. Suhl (Academic Press, New York, 1963), Vol. I, p. 383.
[45] The additional angular indipendent weak signal observed around $g=2$ ($H_{\mathrm{res}}\approx 3300$ Oe) can be attributed to the background and is due to contaminations of the liquid helium.
[46] T. Ogushi, Phys. Rev. **133**, A1098 (1964).
[47] B. J. Klemme, S. E. Brown, P. Wzietek, G. Kriza, P. Batail, D. Jérome, and J. M. Fabre, Phys. Rev. Lett. **75**, 2408 (1995).
[48] L. R. Walker, in *Magnetism*, edited by G. T. Rado and H. Suhl (Academic Press, New York, 1963), Vol. I, p. 299.